STUDY OF STOICHIOMETRIC ETHYLENE AND ETHYLENE/ETHANOL LOW PRESSURE PREMIXED FLAMES USING MASS-SPECTROMETRY WITH SYNCHROTRON PHOTOIONIZATION AND MODELING.

S.A. Yakimov[*], D.A. Knyazkov[*], T.A. Bolshova[*], A.G. Shmakov[*], O.P. Korobeinichev[*], Jzh. Yang[**] and F. Qi[**]
yakimov@kinetics.nsc.ru
[*] Institute of Chemical Kinetics and Combustion, Novosibirsk, Russia
[**] University of Science and Technology of China, Hefei, China

Abstract
Effect of ethanol addition on the species pool in stoichiometric laminar flat flame of ethylene at 30 torr is studied in this work experimentally and by computer modeling. Mole fraction profiles of various stable and labile species including reactants, major products and intermediates measured using molecular beam mass spectrometry with photoionization by VUV synchrotron radiation in $C_2H_4/O_2/Ar$ and $C_2H_4/EtOH/O_2/Ar$ flames are reported. The experimental profiles are compared with those calculated using detailed kinetic mechanism of hydrocarbon and ethanol combustion. Performances and deficiencies of the mechanism in predicting the experimental data are discussed.

Introduction
Oxygen-containing compounds (oxygenates) had recently drawn a lot of attention because of their ability to reduce CO, NOx and soot concentrations in an exhaust gases of various combustion devices when added to a conventional hydrocarbon fuels. Soot formation is undesirable mainly for its negative environmental impact, but it also causes the loss of effectiveness of gas turbines, furnaces, diesel and internal combustion engines, etc. It is essential to understand the chemistry of combustion of hydrocarbon/oxygenate blends to evaluate carbon emissions and efficiency of combustion devices when such blends are used as a fuel. One of the most promising oxygenates is ethanol: tens of billions of gallons per year are produced industrially and the utilization of ethanol as a fuel additive or an individual fuel will eventually grow.

In recent studies, the effect of ethanol additives on the combustion of different hydrocarbons, like *n*-heptane [1, 2], ethane [3], diesel fuel [4], and propylene [5], was investigated experimentally and by numerical modeling. Combustion of ethylene/ethanol mixtures is interesting for a number of reasons and has been studied elsewhere [6-9]. Ethylene is an important intermediate product and is abundant in most of hydrocarbon flames. Thus, ethylene flame may be considered as a simplified model for study of combustion of the conventional fossil-derived hydrocarbon fuels. The studies [1-10] have a common objective: to develop a mechanism that will describe the effect of oxygenated additives (ethanol, particularly) on formation of soot and polyaromatic hydrocarbons (PAHs) in different flames by experimental and numerical study of chemical structure of the flames. The results obtained in these studies appeared to be dependent on experimental conditions: in some cases, ethanol addition resulted in the reduction of PAH concentration, and in other cases, it led to its increase. It has been noted that direction of effect is related to mixing conditions [11]: soot promotion is observed in diffusion flames with ethanol added on the side of fuel, while premixed systems indicates the suppression of soot.

Objectives

We report here measurements of mole fractions of 22 species in two stoichiometric, low pressure 4.0 kPa (30 torr) premixed laminar $C_2H_4/O_2/Ar$ and $C_2H_4/C_2H_5OH/O_2/Ar$ flames. Molecular-beam mass spectrometry with synchrotron photoionization (PI-MBMS) was used to measure mole fractions of stable and labile species. This paper is focused on the effect of ethanol addition on the species pool in ethylene flame. The experimental data are compared in this work with the results of numerical modeling.

Experimental

The experiments were conducted in the National Synchrotron Radiation Laboratory, Hefei, China. Flat laminar premixed flame was stabilized at the horizontally aligned 6 cm diameter McKenna burner under the pressure of 30 torr. A flame sample was extracted from the burning region with a cone-shaped quartz nozzle with 40^o aperture angle and 500 μm orifice diameter. A nickel skimmer was used to cut the central part of the molecular beam, which then entered the ionization chamber where it was exposed to synchrotron VUV radiation. Photoions were collected and analyzed by a reflectron time-of-flight mass spectrometer (RTOF-MS). The synchrotron radiation was taken from two beamlines of the 800 MeV electron storage ring: 1) undulator beamline with 1 m Seya-Namioka monochromator equipped with a 1500 grooves/mm grating, energy resolution $E/\Delta E=1000$, the average photon flux being about 10^{13} photons/s; 2) bend magnet beamline with 1 m Seya-Namioka monochromator equipped with a 1200 grooves/mm grating, energy resolution $E/\Delta E=500$, average photon flux $5x10^{10}$ photons/s. A gas filter with inert gas (Ne or Ar) was used to eliminate higher-order harmonic radiation. Photon flux was measured by SXUV-100 silicon photodiode to normalize ion signals. The experimental setup is described in detail elsewhere [12].

Two stoichiometric flames have been studied: pure ethylene flame ($C_2H_4/O_2/Ar=0.175/0/0.525/0.3$), which was considered as the base flame, and a flame with a 1:1 ratio of ethylene to ethanol ($C_2H_4/EtOH/O_2/Ar = 0.0875/0.0875/0.525/0.3$). In both flames, the flow velocity of the cold (300 K) mixture was maintained at 37.33 cm/s.

The flame temperature was measured with a 0.076-mm-diameter Pt/Pt–13%Rh thermocouple coated with Y_2O_3-BeO anti-catalytic ceramic [13]. The thermocouple was placed at the distance of 15 mm from the sampling cone orifice. Radiation losses were also taken into account.

Ion signal intensities, normalized by the photon flux, were measured and plotted versus: (a) the distance from the burner to the tip of the probe orifice at the constant photon energy (9, 9.5, 10, 10.8, 11.8, 12.3, 13.5, 14.35, 16.2 eV); and (b) photon energy while probe was in the middle of luminous region. The former data provide information about spatial species distribution in flame, the latter give photoionization spectra, which are needed to identify species by their ionization energies. Considering the cooling effect of a molecular beam [16], the errors of IE determination are ±0.05 eV for species with strong signal-to-noise (S/N) ratios and ±0.10 eV for species with weak S/N ratios.

The procedure of mole fraction calculation from ion signal intensities was described by Cool et al. [14] and in our previous work [15]. Briefly, the ion signal recorded for a flame species *i* may be written as

$$S_i(T) = CP_i\sigma_i(E)D_i\Phi_P(E)F(k,T,P), \quad (1)$$

where C is the constant of proportionality, T and $P_i(T)$ are the local flame temperature and spatial pressure of species I; σ_i is the photoionization cross-section at the photon energy E; D_i is the mass discrimination factor for species I; $\Phi_p(E)$ is the photon flux; $F(k, T, P)$ is the empirical instrumental sampling function that relates the molecular beam molar density at the ionization

region to the flame pressure P and the local temperature T; k is the specific heat ratio. The next equation was used to define major species' mole fractions in flame:

$$X_i(T) / X_i(T_0) = [S_i(T) / S_i(T_0)] / FKT(T, T_0), \quad (2)$$

where X_i is the mole fraction of species i, and T_0 refers to the temperature at the burner surface and $FKT(T,T_0)$ is the normalized sampling function

$$FKT(T, T_0) \equiv F(k, T, P) / F(k, T_0, P), \quad (4)$$

which can be constructed by using measurements of signal ratio of argon $S_{Ar}(T)/S_{Ar}(T_0)$. This is suitable for species of entering gases, while the temperature T_F measured at 30 mm from the burner was used for post flame species.

The mole fractions of the other species can be found using following equation:

$$X_i(T) = S_i(T)[X_j(T) / S_j(T)][\sigma_j(E) / \sigma_i(E)][Dj / D_i]. \quad (5)$$

Mass discrimination factors were measured by comparing ion signals in several binary mixtures. Photoionization cross-sections were taken from literature [16-19]. Experimental errors in determination of species mole fractions were mainly due to the uncertainties in PI cross-sections of the species. The mole fraction uncertainty for the stable species was estimated to be about 25% and for radicals mole fractions were determined within a factor of about 2.

Modeling

Kinetic modeling was conducted using the PREMIX code from the CHEMKIN II package. The temperature profile used in calculations was derived from the experimental temperature by lowering it by 100 K [20, 21] and shifting 3.5 mm away from the burner surface in order to take into account the thermocouple's temperature disturbance caused by the probe's cooling effects [22]. Such consideration of the temperature profile perturbation has ensured, as shown below, satisfactory agreement between the measurement results and the calculated concentration profiles of stable species. The detailed kinetic mechanism consisted of two parts: the base mechanism was developed by Frenklach and co-workers [23, 24] and the ethanol oxidation mechanism was borrowed from Marinov [25]. The reactions selected from the ethanol mechanism were the initial reactions of the molecules themselves such as hydrogen abstraction and unimolecular decomposition, along with reactions of the resulting products that eventually produced species present in the base mechanism. The thermodynamic data were also combined to provide the required input data. The resultant mechanism contained 121 species and 708 reactions, of which 20 species and 164 reactions were added from the ethanol mechanism.

The base mechanism includes pyrolysis and oxidation of C_1 and C_2 species, formation of heavy linear hydrocarbons up to C_6 species, formation of benzene and further reactions leading to formation of pyrene, as well as the oxidation pathways of the aromatic species. The odd-carbon-atom formation of the first aromatic ring occurs by the widely accepted combination of propargyl (C_3H_3) radicals, which are treated as an overall single irreversible step with the rate constant fitted to the experimental species profiles of laminar premixed flames of ethane, ethylene and acetylene against which the model was validated [23, 24].

The ethanol mechanism developed by Marinov [25] has been validated against a number of experimental data sets. These include laminar flame speed data, data from a constant volume bomb and counter-flow twin-flame, ignition delay data behind a reflected shock wave, and ethanol oxidation product profiles from a jet-stirred and turbulent flow reactor. Good agreement

between the model and measurements has been observed for five different experimental systems. This mechanism was developed after a thorough review of the kinetics literature.

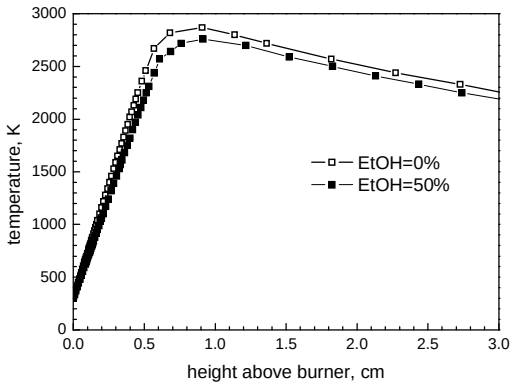

Figure 1. Measured temperature profiles in stoichiometric ethylene and ethylene/ethanol flames.

Results and discussion

Measured temperature profiles are presented in Fig. 1. It can be seen that the replacement of 50% of ethylene by ethanol does not result in a significant change of temperature distribution (the difference is about 100 K). The width of flame zone is about 9 mm in both flames.

Simulated and experimental mole fraction profiles of reactants and major products in both flames are shown in Fig. 2. Some differences observed between experimental and simulated mole fraction profiles of reactants (C_2H_4, C_2H_5OH, O_2) can be associated with the uncertainties in calibration for these species. They were calibrated to match the initial cold-flow concentrations at the burner surface. However, the actual concentrations of the reactants at the burner surface are in fact lower than their fresh mixture concentrations due to diffusion of combustion products from the flame zone to the burner surface. Since the uncertainty of determination of mole fractions of products (CO, CO_2, H_2O) is about 25%, one can see that the agreement between modeled and measured profiles of the products is satisfactory. Despite of the abovementioned quantitative differences between the modeling and experimental results for reactants and major products, the chemical kinetic mechanism used predicts qualitatively well the mole fraction profiles of these species. The mechanism adequately describes the effect of replacement of a part of ethylene with ethanol in fresh gas mixture on the concentrations of these species along the flame zone. In particular, as seen from Fig.2, in the post-flame zone both model and experiment show that in the flame with ethanol CO_2 mole fraction does not change, CO mole fraction is lower, and H_2O mole fraction is higher in comparison with ethylene flame.

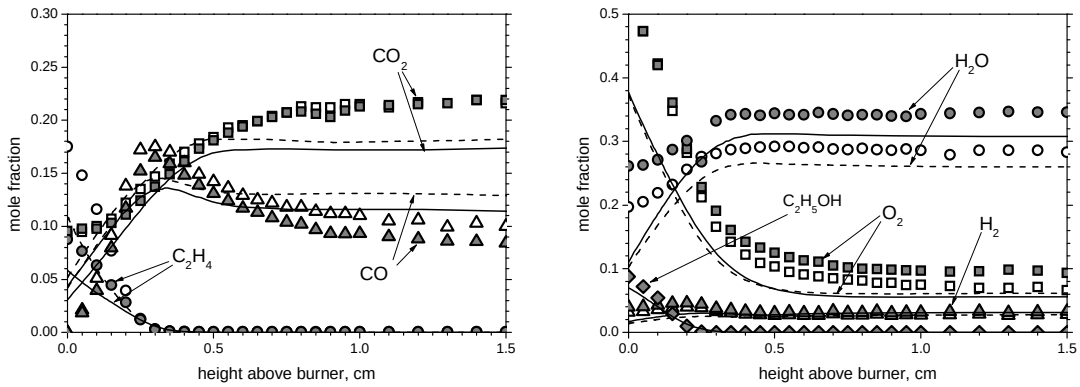

Figure 2. Mole fraction profiles of reactants and products in stoichiometric ethylene and ethylene/ethanol (1:1) flames. Symbols: experiments, lines: modeling. Open symbols and dashed lines are for neat ethylene flame, filled symbols and solid lines are for ethylene/ethanol flame.

Measured and calculated mole fraction profiles of flame intermediates are presented in Figs. 3 and 4. Maximum experimental and calculated concentrations of some of the species are decreased up to 2 times with the change of flame composition from ethylene to ethylene/ethanol. These are 1,3-butadiene C_4H_6, acetylene C_2H_2, allene and propyne C_3H_4, allyl radical C_3H_5, methylketene CH_3CHCO, propargyl radical C_3H_3, and vinylacetylene C_4H_4. For other species, concentrations are increased in both experiment and modeling, these are the products of ethanol oxidation: acetaldehyde and ethenol CH_3CHO, ketene CH_2CO, and acetone C_3H_6O. Acetone (Fig. 4) has no modeling results plotted because it is not presented in the kinetic mechanism used here. Concentration of formaldehyde H_2CO is also increased in modeling, but just slightly reduced in experiment. For methyl radical CH_3 and methane CH_4, a good agreement between experimental and calculated profiles is observed, but the effect of substitution of part of ethylene to ethanol on peak concentration of these species is small.

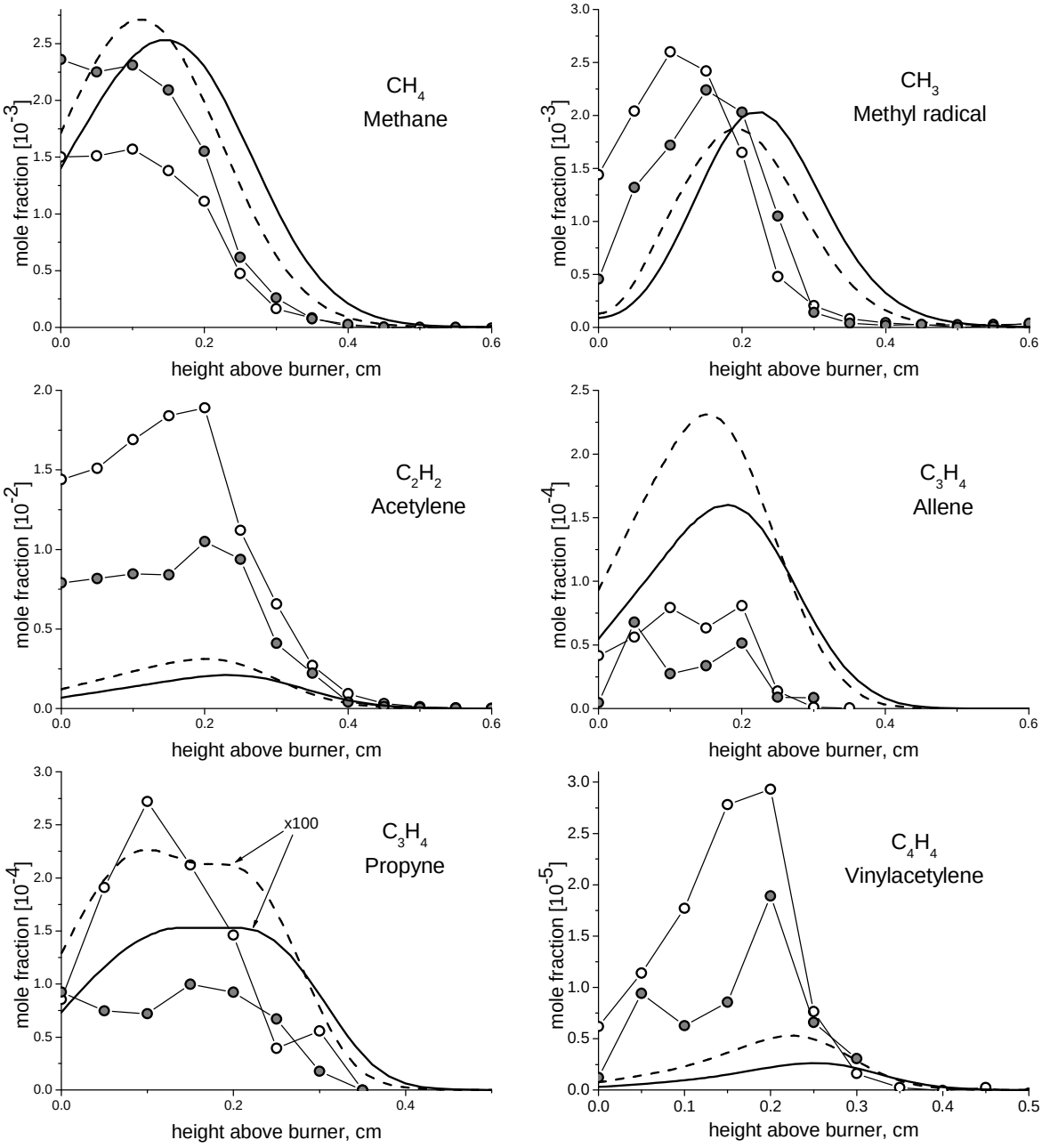

Figure 3. Mole fraction profiles of intermediate species in stoichiometric ethylene and ethylene/ethanol (1:1) flames. Symbols: experiments, lines: modeling. Open symbols and dashed lines are for neat ethylene flame, filled symbols and solid lines are for ethylene/ethanol flame.

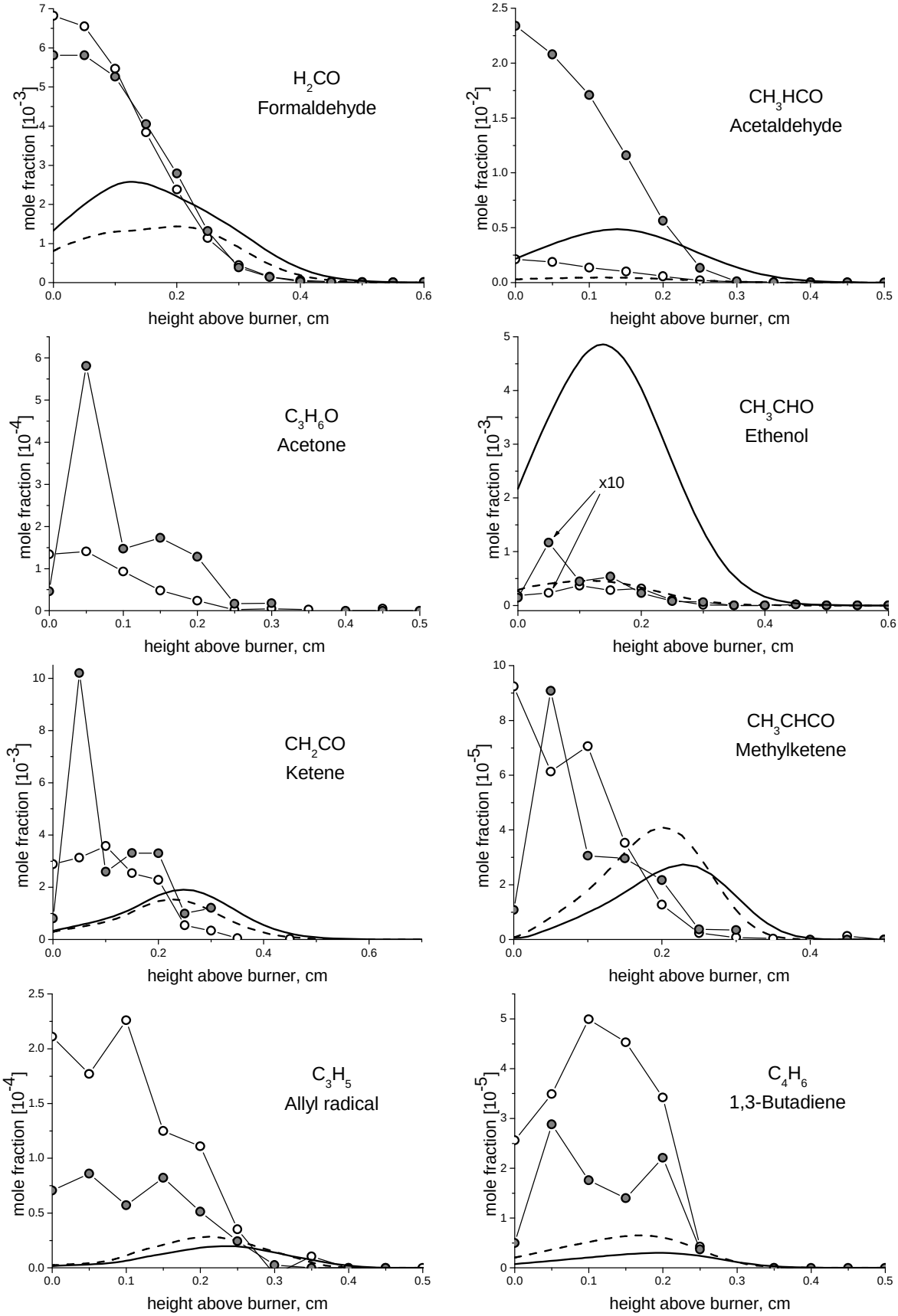

Figure 4. Mole fraction profiles of intermediate species in stoichiometric ethylene and ethylene/ethanol (1:1) flames. Symbols: experiments, lines: modeling. Open symbols and dashed lines are for neat ethylene flame, filled symbols and solid lines are for ethylene/ethanol flame.

It can be seen that the model predicts the concentration of main intermediates qualitatively well. Quantitative discrepancies between experiment and numerical calculations for some of the species indicate the need for further development of the kinetic scheme.

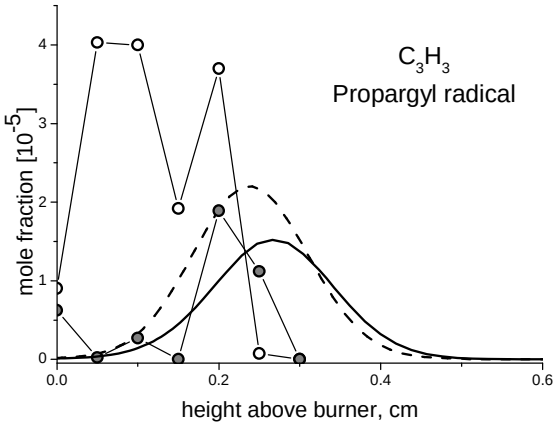

Figure 5. Mole fraction profile of propargyl radical in stoichiometric ethylene and ethylene/ethanol (1:1) flames. Symbols: experiments, lines: modeling. Open symbols and dashed lines are for neat ethylene flame, filled symbols and solid lines are for ethylene/ethanol flame.

Propargyl radical is known as a benzene precursor in hydrocarbon flames. As can be seen from Fig. 5, its concentration decreases 2 times when half of ethylene in the fresh gas mixture is substituted with ethanol. It is qualitatively consistent with our previous data obtained in fuel-rich (φ=2.0) conditions [15] and indicates that ethanol addition leads to reduction of soot precursors in stoichiometric flame. Benzene was not detected in the present experiments because its concentration was below the detection limit even in the flame of neat ethylene.

Conclusion

In this study the effect of ethanol addition on the species pool in premixed burner-stabilized ethylene flames at 4.0 kPa (30 torr) was investigated. PI-MBMS measurements and 1D kinetic modeling of mole fraction profiles of reactants, major products and intermediate species were performed in stoichiometric $C_2H_4/O_2/Ar$ and $C_2H_4/EtOH/O_2/Ar$ flames. Comparison of the computed and measured concentration profiles of different species (reactants, major products, and intermediate C_1-C_4 hydrocarbons) has shown that the chemical kinetic mechanism used qualitatively describes the structure of the flames and predicts satisfactory the general trend of the influence of ethanol addition on changing concentrations of major intermediate species in the flames. Some quantitative discrepancies between the modeling and measurement data were observed. This indicates the need of improving the mechanism, and this is the goal of our future work. It has been established both experimentally and by way of modeling that the concentration of propargyl radicals, the main benzene precursors, is lower in the flame of the fuel mixture ethylene/ethanol than in the ethylene flame, indicating that ethanol contributes to suppression of formation of soot precursors.

References

[1] F. Inal, S.M. Senkan, *Combust. Sci. Technol.* 174: 1–19 (2002).
[2] T. Kitamura, T. Ito, J. Senda, H. Fujimoto, *JSAE Rev.* 22: 139-145 (2001).
[3] K.H. Song, P. Nag, T.A. Litzinger, D.C. Haworth, *Combust. Flame* 135: 341–349 (2003).
[4] L. Xingcai, H. Zhen, Z. Wugao, L. Degang, *Combust. Sci. Technol.* 176: 1309–1329(2004).

[5] K. Kohse-Höinghaus, P. Oßwald, U. Struckmeier, T. Kasper, N. Hansen, C.A. Taatjes, J. Wang, T.A. Cool, S. Gon and P.R. Westmoreland, *Proc. Comb. Inst.* 31: 1119-1127 (2007).
[6] K.L. McNesby, A.W. Miziolek, T. Nguyen, F.C. Delucia, R.R. Skaggs, T.A. Litzinger, *Combust. Flame* 142: 413–427 (2005).
[7] J. Wu, K.H. Song, T. Litzinger, S.-Y. Lee, R. Santoro, M. Linevsky, M. Colket, D. Liscinsky, *Combust. Flame* 144: 675–687 (2006).
[8] C.S. McEnally, L.D. Pfefferle, *Proc. Combust. Inst.* 31: 603–610 (2007).
[9] B.A.V. Bennett, C.S. McEnally, L.D. Pfefferle, M.D. Smooke, M.B. Colket, *Comb. Flame* 156: 1289–1302 (2009).
[10] T. Ni, S.B. Gupta, R.J. Santoro, *Proc. Combust. Inst.* 25: 585-592 (1994).
[11] T. Litzinger, M. Colket, M. Kahandawala, V. Katta, S. -Y. Lee, D. Liscinsky, K. McNesby, R. Pawlik, M. Roquemore, R. Santoro, S. Sidhu, S. Stouffer, J. Wu, *Combust. Sci. Technol.* 181: 310-328 (2009).
[12] F. Qi, R. Yang, B. Yang, et al., *Rev. Sci. Instrum.* 77: 084101 (2006).
[13] J.H. Kent, *Combust. Flame* 14: 279–281 (1970).
[14] T.A. Cool, K. Nakajima, K.A. Taatjes, A. McIlroy, P.R. Westmoreland, M.E. Law, A. Morel, *Proc. Combust. Inst.* 30: 1681–1688 (2005).
[15] O.P. Korobeinichev, S.A. Yakimov , D.A. Knyazkov, T.A. Bolshova , A.G. Shmakov , Jzh. Yang, F. Qi, *Proc. Combust. Inst.* 33: 569-576 (2011).
[16] T.A. Cool, J.Wang, K.Nakajima, C.A.Taatjes, A. McIlroy, *Int. J. Mass Spectrom.* 247: 18–27 (2005).
[17] T.A. Cool, K. Nakajima, T.A. Mostefaoui, F. Qi, A. McIlroy, P.R. Westmoreland, M.E. Law, L. Poisson, D.S. Peterka, M. Ahmed, *J. Chem. Phys.* 119: 8356–8365 (2003).
[18] J.C. Robinson, N.E. Sveum, D.M. Neumark, *J. Chem. Phys.* 119: 5311–5314 (2003).
[19] J.C. Robinson, N.E. Sveum, D.M. Neumark, *Chem. Phys. Lett.* 383: 601–605 (2004).
[20] Y. Li, L. Wei, Z. Tian, B. Yang, J. Wang, T. Zhang, F. Qi., *Combust. Flame* 152: 336-359 (2008).
[21] P. Desgroux, L. Gasnot, J.F. Pauwels, L.R. Sochet, *Appl. Phys. B* 61: 401–407 (1995).
[22] A. T. Hartlieb, B. Atakan, K. Kohse-Höinghaus, *Combust. Flame* 121: 610-624 (2000).
[23] J. Appel, H. Bockhorn, M.Y. Frenklach, *Combust. Flame* 121: 122-136 (2000).
[24] H. Wang, M. Frenklach, *Combust. Flame* 110: 173-221 (1997).
[25] N.M. Marinov, *Inter. J. of Chem. Kin.* 31: 183-220 (1998).